A time-frequency method for nonstationary jammer suppression in DSSS systems

Slobodan Djukanović, *Student Member, IEEE*, Ljubiša Stanković, *Senior Member, IEEE*, and Miloš Daković, *Member, IEEE*

Abstract — **In this paper, we deal with the nonstationary jammer suppression in direct sequence spread spectrum (DSSS) communication systems by using time-frequency (t-f) methods. In specific, we developed a DSSS receiver based on the local polynomial Fourier transform (LPFT). The LPFT is known for its possibility to optimally concentrate the jammer in the t-f plane. Time-varying filtering is implemented in the optimal LPFT domain. The LPFT receiver is derived in matrix form and its optimization is performed, taking into consideration the influence of the filtering function on the received signal. The conventional (suboptimal) and optimal LPFT receivers are compared by simulations carried out on the received signal corrupted by different types of FM interferences. A receiver based on the standard short-time Fourier transform (STFT) is considered as a special case of the LPFT receiver and its performance is assessed simultaneously with the LPFT receiver, both in the conventional and optimal case.**

Index terms — **Filtering, Fourier transform, spread spectrum (SS) communications, time-frequency (t-f) analysis.**

I. Introduction

In direct sequence spread spectrum (DSSS) systems, pseudo-noise (PN) code sequence modulates the information signal before its transmission. Since the PN sequence varies faster than the information signal, the modulation expands its spectrum $G=T_b/T_c$ times, where G is the processing gain, T_b is duration of the information symbol (bit) and T_c is duration of the PN sequence symbol (chip). DSSS systems exhibit narrowband and broadband interference resistance, since the information signal is restored to its original frequency band (despread) by multiplying the received signal with a synchronized replica of the PN sequence at the receiver side, while everything else is additionally spread. In this way, despreading provides resistance to the multipath fading, since it also spreads all versions of the SS signal delayed by more than T_c. Moreover, since the PN sequence is known only to the transmitter and receiver, the privacy of the transmission is provided.

The interference (jammer) may be superimposed on the transmitted signal intentionally, as in military communications, or unintentionally, as in commercial communications. Low power interferences are substantially neutralized by despreading, but signals corrupted by high power interferences have to be preprocessed before the correlation at the receiver side is done. Numerous interference suppression techniques have been proposed in order to enhance the performance of the DSSS receiver in severe interfering environment [1]–[8]. Most of these techniques use the interference suppression filter before the correlator in the receiver scheme. This is usually an adaptive filter which exploits the pseudo-white properties of SS signals. Recently, time-frequency (t-f) based methods have appeared, which are very effective in improving the receiver's performance when the desired signal is corrupted by broadband interferences with narrowband instantaneous bandwidths [1], [3], [4], [7], [8].

Among significant contributions, several papers will be mentioned. Amin and coauthors [1]–[3] proposed several methods that use the adaptive filtering for the nonstationary interference suppression. The instantaneous frequency (IF) of the interference can be successfully estimated by means of t-f distributions and used to construct a finite impulse response filter that reduces the interference power with a minimum possible distortion of the desired signal [1]. The optimum receiver that implements the short-time Fourier transform (STFT) interference excision system is developed in [3]. Another t-f method, the generalized Wigner-Hough transform, has been proposed for the multiple interferences rejection [4]. The fractional Fourier transform can be a useful tool in case of linear FM interferences [5]. A comprehensive analysis of DFT-based frequency excision algorithms has been presented in [6]. A nonparametric approach for the multiple jammers excision by using the local polynomial Fourier transform (LPFT) has been presented in [7].

This paper presents an optimization of the method proposed in [7]. In particular, introduced time-varying filtering procedure uses a binary mask to remove the jammer, which was previously optimally concentrated in the t-f plane using the LPFT [10]. The binary mask is a two-dimensional function of time and frequency with values 0 (jammer exists in (t,f)) and 1 (jammer does not exist in (t,f)). However, the binary mask introduces a distinction between the received PN sequence and original one, making their correlation suboptimal. This paper develops an optimal LPFT-based receiver which takes into account the distortion effect of the binary mask on the received PN sequence. This receiver is shown to depend on the analysis window, binary excision mask, white noise

The authors are with the Faculty of Electrical Engineering, University of Montenegro, 81000 Podgorica, Montenegro (e-mail: slobdj@ac.me; milos@ac.me; ljubisa@ac.me).

power and optimal LPFT coefficients.

The paper is organized as follows. Section II presents the conventional LPFT receiver for the nonstationary jammer excision in matrix form, along with simple signal synthesis procedure. The optimal LPFT receiver is developed in Section III. The original PN sequence at the receiver side is modified so that it optimally corresponds to distorted received PN sequence. The modification is obtained by means of a multiplicative matrix **C**. The LPFT receiver with maximum output signal-to-noise ratio (SNR_{out}) is referred to as the optimal receiver and the matrix **C** that maximizes SNR_{out} is calculated. In Section IV, the performance of the proposed optimized receiver is evaluated by simulations carried out for two types of simulated FM jammers with varying parameters, linear and sinusoidal FM jammers.

II. Conventional Local Polynomial Fourier Transform Receiver

The DSSS signal description can be found in [7] and [12]. The baseband received signal $x(n)$ contains three mutually uncorrelated sequences as follows:

$$x(n) = s(n) + j(n) + \xi(n), \tag{1}$$

where $s(n)$ is the SS sequence of unit amplitude, $j(n)$ is the jammer sequence and $\xi(n)$ is the additive white Gaussian noise sequence with zero mean and variance σ_ξ^2. For the SS signal of unit amplitude, we have $SNR=-20\log_{10}(\sigma_\xi)$. The jammer can be analytically expressed as

$$j(n) = a_j \cos(\varphi(n)), \tag{2}$$

where $\varphi(n)$ is the phase and a_j is the amplitude of the jammer. The jammer-to-signal ratio (JSR) is defined as $JSR=10\log_{10}(P_j/P_s)$, where P_j and P_s represent the power of the jammer and SS signal, respectively [12], [14]. Besides, the SS signal characterized by one sample per chip is assumed, when perfectly flat spectrum of the SS signal is obtained [6]. Therefore, $s(n)$ equals $p(n)$ when bit "1" is transmitted and $-p(n)$ when "−1" is transmitted, where $p(n)$ is the PN sequence with the length L and the following statistical properties:

$$E[p(n)] = 0 \quad \text{and} \quad E[p(n)p^*(m)] = \delta(n-m). \tag{3}$$

In (3), E[•] denotes the statistical expectation, $\delta(n)$ is the Dirac delta function and "*" is the conjugation operator.

The LPFT has been introduced in the t-f analysis by Katkovnik [7], [10], and the Mth order discrete form of the LPFT of the sequence $x(n)$ is defined by

$$\mathrm{LPFT}(n,k) = \sum_{m=-N/2}^{N/2-1} x(n+m)w(m)e^{-j\sum_{i=1}^{M}\omega_i\frac{m^{i+1}}{(i+1)!}}e^{-j\frac{2\pi}{N}mk}, \tag{4}$$

where $w(m)$ represents the analysis window, N is the number of frequency bins and ω_i is the ith transform parameter. The LPFT can be easily calculated using the FFT procedure. We will assume that the number of frequency bins equals L [3]. As (4) indicates, the LPFT of the received signal can be calculated analogously to the STFT, i.e., by sliding the analysis window $w(m)$ over the modulated received signal

$$x(n+m)e^{-j\sum_{i=1}^{M}\omega_i\frac{m^{i+1}}{(i+1)!}}$$

and implementing the FFT procedure on the product of the modulated signal and window at the current position.

In order to analyze the LPFT receiver, equation (4) will be expressed in matrix form. First, the zero-padding of the sequence x is performed by concatenating $N/2$ zeros to both the beginning and the end of x, thus creating a sequence x_z. Then, the $N\times N$ matrix **X** is formed as

$$\mathbf{X} = \begin{bmatrix} x_z(1)\Theta(1,1) & x_z(2)\Theta(1,2) & \cdots & x_z(N)\Theta(1,N) \\ x_z(2)\Theta(2,1) & x_z(3)\Theta(2,2) & \cdots & x_z(N+1)\Theta(2,N) \\ \vdots & \vdots & \ddots & \vdots \\ x_z(N)\Theta(N,1) & x_z(N+1)\Theta(N,2) & \cdots & x_z(2N-1)\Theta(N,N) \end{bmatrix}, \tag{5}$$

where **Θ** is the $N\times N$ matrix defined as

$$\Theta(n,m) = e^{-j\sum_{i=1}^{M}\omega_i(n)\frac{(m-N/2-1)^{i+1}}{(i+1)!}},$$

where $\omega_i(n)$ is the ith LPFT parameter at the nth window position. Also, define matrix

$$\mathbf{W} = \begin{bmatrix} w(1)W_N^0 & w(1)W_N^0 & \cdots & w(1)W_N^0 \\ w(2)W_N^0 & w(2)W_N^1 & \cdots & w(2)W_N^{N-1} \\ \vdots & \vdots & \ddots & \vdots \\ w(N)W_N^0 & w(N)W_N^{N-1} & \cdots & w(N)W_N^{(N-1)^2} \end{bmatrix}_{N\times N} \tag{6}$$

with $W_N = e^{-j2\pi/N}$. Now, the LPFT of the received signal $x(n)$ may be written in matrix form as

$$\mathbf{LPFT} = \mathbf{X}\,\mathbf{W}. \tag{7}$$

The LPFT is a linear transform and reconstruction (synthesis) of the signal from its LPFT at the time instant n is obtained simply by summing elements of the nth row of matrix **LPFT** [7], i.e.

$$x'(n) = \frac{1}{N}\sum_{k=1}^{N}\mathrm{LPFT}(n,k) \tag{8}$$

where $x'(n)$ represents the reconstructed signal. In (8), $w(0)=1$ is assumed.

The LPFT parameters ω_i for $i=1,2,...,M$ are calculated so as to optimally concentrate the jammer in the t-f plane for given analysis window. To that aim, an order adaptive algorithm is developed in [7] and it is shown to keep the calculation complexity at a relatively low level. Furthermore, it is shown that the second-order LPFT produces results almost independent of the parameters of FM interferences, thus preventing the need for a time-consuming calculation of higher-order LPFTs[1]. The jammer excision is then obtained in the optimal LPFT domain by removing its t-f signature via a binary mask **B**, which is a matrix with the same dimensions as **LPFT** and values 0 in all t-f points (n,k) of the LPFT corrupted by the jammer and 1 otherwise. The synthesis is then

[1] For a stationary jammer, the STFT and the optimal LPFT are the same, and therefore their calculation complexities coincide. For a linear FM jammer, the optimal LPFT complexity exceeds the STFT complexity for a number of operations required by relations (16)–(19) given in [7]. Finally, for a highly nonstationary jammer, such as sinusoidal FM jammer, the optimal LPFT calculation requires an additional number of operations for the iterative optimization of the second order parameter.

performed on the masked LPFT to recover the jammer-free desired signal as follows:

$$\begin{aligned} x'(n) &= \frac{1}{N}\sum_{k=1}^{N} \mathrm{LPFT}(n,k)B(n,k) \\ &= \frac{1}{N}\sum_{k=1}^{N}\left[\sum_{l=1}^{N} X(n,l)W(l,k)\right]B(n,k) \\ &= \frac{1}{N}\sum_{l=1}^{N} X(n,l)\sum_{k=1}^{N} W(l,k)B(n,k). \end{aligned} \tag{9}$$

Denoting the product of $\mathbf{W}$ and $\mathbf{B}^T$ as $\mathbf{W_B}=\mathbf{WB}^T$, where "$T$" denotes the transposition operator, we obtain

$$\begin{aligned} x'(n) &= \frac{1}{N}\sum_{l=1}^{N} X(n,l)W_B(l,n) \\ &= \frac{1}{N}\sum_{l=1}^{N} (P(n,l)+\Xi(n,l))W_B(l,n), \end{aligned} \tag{10}$$

which implies that the main diagonal of the matrix product $\mathbf{XW_B}$ represents the scaled reconstructed signal. In addition, since it is assumed that the excision mask $\mathbf{B}$ completely removes the jammer[2] [3], the only two components of the matrix $\mathbf{X}$ that will be hereafter considered are the PN matrix $\mathbf{P}$ and the noise matrix $\mathbf{\Xi}$, which can be obtained from (5) by setting $x_z(n)=p_z(n)$ and $x_z(n)=\xi_z(n)$, respectively. The sequences $p_z(n)$ and $\xi_z(n)$ are the zero-padded PN sequence $p(n)$ and zero-padded noise sequence $\xi(n)$, respectively.

Naturally, if the LPFT is modified by the excision mask, the synthesized PN sequence will no longer coincide with the original one. More precisely, the synthesized PN sequence becomes the time-varying convolution between the original PN sequence and binary mask.

In particular, by setting all elements of the matrix $\mathbf{\Theta}$ to 1, i.e., each ω_i to 0, the LPFT receiver becomes the STFT receiver, so the STFT receiver can be considered as a special case of the LPFT receiver. The comparison between the conventional STFT and LPFT receivers' performances for received signals corrupted by nonstationary FM interferences with variable parameters is drawn in [7].

III. Optimal Local Polynomial Fourier Transform Receiver

For detection of the information symbol, the decision variable d is formed as the correlation of the reconstructed signal $x'(n)$ and modified receiver PN sequence $\mathbf{q}=[q(1),q(2),\ldots,q(N)]$, that is

$$d = \sum_{n=1}^{N} x'(n)q(n). \tag{11}$$

The sequence $\mathbf{q}$ and the original one $\mathbf{p}$ will be related through the $N\times N$ matrix $\mathbf{C}$, i.e., $\mathbf{q}=\mathbf{Cp}$. The conventional receiver is obtained by setting $\mathbf{C}=\mathbf{I}_{N\times N}$, or $\mathbf{q}=\mathbf{p}$, where $\mathbf{I}_{N\times N}$ is the $N\times N$ identity matrix. The correlation performed between $x'(n)$ and $\mathbf{q}=\mathbf{p}$ produces suboptimal results since it does not take into account the modification of the received PN sequence induced by the binary mask $\mathbf{B}$.

The SNR at the output of the receiver correlator [13],

$$\mathrm{SNR}_{\mathrm{out}} = \frac{E^2[d]}{\mathrm{Var}[d]}, \tag{12}$$

depends on the matrix $\mathbf{C}$. The receiver with maximal $\mathrm{SNR}_{\mathrm{out}}$ will be referred to as the optimal receiver and the matrix $\mathbf{C}$ that maximizes $\mathrm{SNR}_{\mathrm{out}}$ will be herein determined.

We will start with $E[d]$.

$$\begin{aligned} E[d] &= \frac{1}{N}E\left[\sum_{n=1}^{N}\left(\sum_{k=1}^{N} X(n,k)W_B(k,n)\right)q(n)\right] \\ &= \frac{1}{N}\sum_{n=1}^{N}\sum_{k=1}^{N} E[X(n,k)q(n)]W_B(k,n) \\ &= \frac{1}{N}\sum_{n=1}^{N}\sum_{k=1}^{N} E\left[X(n,k)\sum_{i=1}^{N} C(n,i)p(i)\right]W_B(k,n) \\ &= \frac{1}{N}\sum_{n,k,i=1}^{N} C(n,i)E[X(n,k)p(i)]W_B(k,n). \end{aligned} \tag{13}$$

To shorten the notation, we introduced the abbreviated form of the triple summation in (13). Furthermore, since $E[\Xi(n,k)p(i)]=0$, $E[d]$ reduces to

$$E[d] = \frac{1}{N}\sum_{n,k,i=1}^{N} C(n,i)E[P(n,k)p(i)]W_B(k,n). \tag{14}$$

Since $P(n,k)=p(n+k-N/2-1)\Theta(n,k)$, we get

$$E[P(n,k)p(i)] = \delta\left(i-n-k+\frac{N}{2}+1\right)\Theta(n,k)$$

and therefore

$$E[d] = \frac{1}{N}\sum_{n,k,i=1}^{N} C(n,i)\delta\left(i-n-k+\frac{N}{2}+1\right)\Theta(n,k)W_B(k,n). \tag{15}$$

Introducing the $N\times N$ matrix $\mathbf{S}$ with

$$S(i,n) = \sum_{k=1}^{N}\delta\left(i-n-k+\frac{N}{2}+1\right)\Theta(n,k)W_B(k,n), \tag{16}$$

we obtain

$$E[d] = \frac{1}{N}\sum_{n=1}^{N}\sum_{k=1}^{N} C(n,i)S(i,n). \tag{17}$$

Define

$$\mathbf{C_1^H} = [\mathbf{c_1}\ \mathbf{c_2}\ \cdots\ \mathbf{c_N}]_{1\times N^2} \quad \text{and} \quad \mathbf{S_1} = \begin{bmatrix} \mathbf{s_1} \\ \mathbf{s_2} \\ \vdots \\ \mathbf{s_N} \end{bmatrix}_{N^2\times 1} \tag{18}$$

where the superscript "H" denotes the Hermitian transposition, $\mathbf{c_i}$ is the $1\times N$ vector (the ith row of $\mathbf{C}$), $\mathbf{s_i}$ is the $N\times 1$ vector (the ith column of $\mathbf{S}$) and $i=1,2,\ldots,N$. Now $E[d]$ can be expressed as

$$E[d] = \frac{1}{N}\mathbf{C_1^H S_1}. \tag{19}$$

The derivation of $\mathrm{Var}[d]$ will be omitted here, only the final matrix form will be given. The derivation details are given in [8]. The final matrix form of $\mathrm{Var}[d]$ is

[2] Strictly speaking, the jammer cannot be completely removed from the t-f plane because of finite length of the analysis window. However, for a given time instant, we can neglect the jammer power concentrated in sidelobes of its spectrum, especially when windows with highly suppressed sidelobes are used (e.g., Kaiser window [7]). Therefore, in this paper, to completely remove the jammer means to excise only its main lobe.

$$\mathrm{Var}[d] = \mathbf{C}_1^H \left((1+\sigma_\xi^2)\mathbf{T}_1 + \mathbf{S}_2\mathbf{S}_3^T - 2\mathbf{T}_2 \right)\mathbf{C}_1, \quad (20)$$

where the matrices $\mathbf{T}_1$, $\mathbf{T}_2$, $\mathbf{S}_2$ and $\mathbf{S}_3$ are defined below.

$$\mathbf{T}_1 = \begin{bmatrix} \mathbf{t}_{11}^1 & \mathbf{t}_{12}^1 & \cdots & \mathbf{t}_{1N}^1 \\ \mathbf{t}_{21}^1 & \mathbf{t}_{22}^1 & \cdots & \mathbf{t}_{2N}^1 \\ \vdots & \vdots & \ddots & \vdots \\ \mathbf{t}_{N1}^1 & \mathbf{t}_{N2}^1 & \cdots & \mathbf{t}_{NN}^1 \end{bmatrix}_{N^2\times N^2} \quad (21)$$

where

$$\mathbf{t}_{n_1 n_2}^1 = T(n_1, n_2)\mathbf{I}_{N\times N} \quad (22)$$

and

$$T(n_1,n_2) = \sum_{k_1,k_2=1}^{N} \delta(n_1+k_1-n_2-k_2)\Theta(n_1,k_1) \times W_B(k_1,n_1)\Theta^*(n_2,k_2)W_B^*(k_2,n_2). \quad (23)$$

Next, the matrix $\mathbf{T}_2$ satisfies

$$\mathbf{T}_2 = \begin{bmatrix} \mathbf{t}_{11}^2 & \mathbf{t}_{12}^2 & \cdots & \mathbf{t}_{1N}^2 \\ \mathbf{t}_{21}^2 & \mathbf{t}_{22}^2 & \cdots & \mathbf{t}_{2N}^2 \\ \vdots & \vdots & \ddots & \vdots \\ \mathbf{t}_{N1}^2 & \mathbf{t}_{N2}^2 & \cdots & \mathbf{t}_{NN}^2 \end{bmatrix}_{N^2\times N^2} \quad (24)$$

where

$$\mathbf{t}_{n_1 n_2}^2 = \begin{bmatrix} R(1,k_1,k_2) & 0 & \cdots & 0 \\ 0 & R(2,k_1,k_2) & \cdots & 0 \\ \vdots & \vdots & \ddots & \vdots \\ 0 & 0 & \cdots & R(N,k_1,k_2) \end{bmatrix}_{N\times N} \quad (25)$$

and

$$R(i,n_1,n_2) = \sum_{k_1,k_2=1}^{N} \delta(n_1+k_1-n_2-k_2) \times\delta(n_1+k_1-N/2-i-1) \times\Theta(n_1,k_1)W_B(k_1,n_1)\Theta^*(n_2,k_2)W_B^*(k_2,n_2). \quad (26)$$

Finally, $\mathbf{S}_2$ and $\mathbf{S}_3$ are the $N^2\times N^2$ matrices defined as

$$\mathbf{S}_2 = \begin{bmatrix} \mathbf{S}^* & \mathbf{0} & \cdots & \mathbf{0} \\ \mathbf{0} & \mathbf{S}^* & \cdots & \mathbf{0} \\ \vdots & \vdots & \ddots & \vdots \\ \mathbf{0} & \mathbf{0} & \cdots & \mathbf{S}^* \end{bmatrix} \quad (27)$$

$$\mathbf{S}_2 = \begin{bmatrix} \mathbf{s}_1 & \mathbf{0} & \cdots & \mathbf{0} & \mathbf{s}_2 & \mathbf{0} & \cdots & \mathbf{0} & \cdots & \mathbf{s}_N & \mathbf{0} & \cdots & \mathbf{0} \\ \mathbf{0} & \mathbf{s}_1 & \cdots & \mathbf{0} & \mathbf{0} & \mathbf{s}_2 & \cdots & \mathbf{0} & \cdots & \mathbf{0} & \mathbf{s}_N & \cdots & \mathbf{0} \\ \vdots & \vdots & \ddots & \vdots & \vdots & \vdots & \ddots & \vdots & \cdots & \vdots & \vdots & \ddots & \vdots \\ \mathbf{0} & \mathbf{0} & \cdots & \mathbf{s}_1 & \mathbf{0} & \mathbf{0} & \cdots & \mathbf{s}_2 & \cdots & \mathbf{0} & \mathbf{0} & \cdots & \mathbf{s}_N \end{bmatrix}. \quad (28)$$

In (27), $\mathbf{0}$ represents the $N\times N$ zero matrix, whereas in (28) it represents the $N\times 1$ zero vector.

Finally, the SNR at the output of the receiver correlator is

$$\mathrm{SNR}_{\mathrm{out}} = \frac{\mathbf{C}_1^H \mathbf{S}_1 \mathbf{S}_1^H \mathbf{C}_1}{\mathbf{C}_1^H \left((1+\sigma_\xi^2)\mathbf{T}_1 + \mathbf{S}_2\mathbf{S}_3^T - 2\mathbf{T}_2 \right)\mathbf{C}_1} = \frac{\mathbf{C}_1^H \mathbf{Z} \mathbf{C}_1}{\mathbf{C}_1^H \mathbf{Y} \mathbf{C}_1}, \quad (29)$$

where $\mathbf{Z}$ and $\mathbf{Y}$ are the $N^2\times N^2$ matrices defined by

$$\mathbf{Z} = \mathbf{S}_1\mathbf{S}_1^H$$
$$\mathbf{Y} = (1+\sigma_\xi^2)\mathbf{T}_1 + \mathbf{S}_2\mathbf{S}_3^T - 2\mathbf{T}_2. \quad (30)$$

The final form of $\mathrm{SNR}_{\mathrm{out}}$ in (29) corresponds to the Rayleigh quotient. Since the matrices $\mathbf{T}_1$, $\mathbf{S}_2\mathbf{S}_3^T$ are $\mathbf{T}_2$ are Hermitian, $\mathbf{Y}$ and $\mathbf{Y}^{1/2}$ are also Hermitian, allowing us to define a vector $\hat{\mathbf{C}}_1^H = \mathbf{Y}^{1/2}\mathbf{C}_1$ and to rewrite (29) as

$$\mathrm{SNR}_{\mathrm{out}} = \frac{\hat{\mathbf{C}}_1^H \left[(\mathbf{Y}^{-1/2})^H \mathbf{Z} \mathbf{Y}^{-1/2} \right] \hat{\mathbf{C}}_1}{\hat{\mathbf{C}}_1^H \hat{\mathbf{C}}_1}. \quad (31)$$

The Rayleigh quotient states that $\mathrm{SNR}_{\mathrm{out}}$ reaches its maximum when $\hat{\mathbf{C}}_1$ is an eigenvector of the $N^2\times N^2$ matrix $(\mathbf{Y}^{-1/2})^H \mathbf{Z} \mathbf{Y}^{-1/2}$ corresponding to its largest eigenvalue. We will denote such a vector as $\hat{\mathbf{C}}_{\mathbf{1max}}$. The optimal correlator is then obtained by rearranging the $N^2\times 1$ optimal vector

$$\mathbf{C}_{\mathbf{1opt}} = \mathbf{Y}^{-1/2}\hat{\mathbf{C}}_{\mathbf{1max}} \quad (32)$$

back into the $N\times N$ matrix $\mathbf{C}$ according to (18).

The equations (29)–(32) and the previous analysis show that the optimal LPFT receiver depends on the analysis window used in the LPFT calculation, optimal LPFT parameters obtained in the jammer concentration procedure, binary excision mask and noise variance σ_ξ^2. The block diagram of the optimal LPFT receiver is shown in Fig. 1. The variance estimation procedure is given in [15]. The conventional LPFT receiver is simply obtained by bypassing the PN sequence modification block (dashed-line).

IV. Simulations

Example 1: To compare the conventional and the optimal LPFT receiver, we calculated the corresponding $\mathrm{SNR}_{\mathrm{out}}$ values for two different excision cases. In the first case, the binary mask cancels frequency slices in the middle of both the positive and negative part of the spectrum (stationary jammer case), from 0 to 10 slices. We begin with the central frequency, and then cancel one adjacent upper frequency, one adjacent lower frequency and so forth. In the second case, the binary mask cancels diagonal slices of both the positive and negative part of the spectrum (linear FM jammer case), from 0 to 10 slices. We begin with the main diagonal, and then cancel one adjacent upper diagonal, one adjacent lower diagonal and so forth. In both cases, the length of the PN sequence is 32, the Hanning window with 32 samples is used and σ_ξ^2=2. In addition, numerical SNR values are calculated according to (12) over 20000 realizations of the decision variable d. The obtained analytical $\mathrm{SNR}_{\mathrm{out}}$ curves are shown in Fig. 2, along with the corresponding numerical values shown with triangles. In the first excision case, all the LPFT parameters in $\mathbf{\Theta}$ are set to 0, since this case corresponds to the stationary interference excision, i.e., the LPFT and STFT receiver coincide. In the second case, only ω_1 parameters were non-zero, since this case corresponds to the linear FM interference excision. Furthermore, ω_1 is constant and set to a predefined value at which the interference that diagonally sweeps the entire t-f plane (i.e., IF trajectory of the interference coincides with the main diagonal of the positive part of the LPFT spectrum) is optimally concentrated.

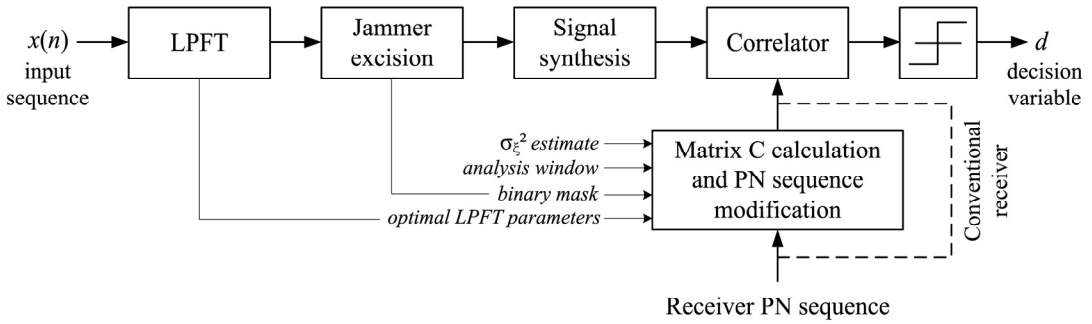

Fig. 1. Block diagram of the optimal LPFT receiver. The conventional receiver is obtained when no modification of the receiver PN sequence is performed (dashed line).

With this setup, the LPFT also produces the same SNR values as the STFT receiver, which is quite straightforward to prove analytically. Nevertheless, for given nonstationary jammer, the LPFT will always produce better results, since it optimally concentrates the jammer in the t-f plane and therefore excises less number of diagonals. It is evident from Fig. 2 that the optimal receiver is less immune to the frequency slices excision than to the diagonal slices excision. This is due to the fact that by removing a single frequency we permanently lose the information component at that frequency, while with removing a single diagonal the removed frequency bin at one time instant is still available at another one.

In the following examples, two types of simulated monocomponent jammers with variable parameters are considered, linear and sinusoidal FM jammer. Analytically obtained SNR_{out} curves are numerically confirmed over 20000 realizations of the decision variable d, while BER values are computed over 20 million runs. As in the first example, the PN sequence length is L=32, the Hanning window with 32 samples is used as the analysis window and σ_ξ^2=2. Besides, we point out that, for each value of the considered jammer parameter, the excision matrix $\mathbf{B}$ (and therefore $\mathbf{C_{1opt}}$) is not determined for each run separately, but only once, for the first realization of the STFT and LPFT of the received signal. Therefore, for each value of the considered jammer parameter, the optimal LPFT parameters are also calculated only in the first run and used in all other runs.

Example 2: In this example, we assess performances of the conventional and optimal STFT and LPFT receivers when the desired signal is corrupted by a linear FM jammer with variable modulation index (chirp rate). The jammer is characterized by JSR=30dB and its chirp rate varies from 0 (a pure sinusoid in the middle of the spectrum) to a value at which it sweeps the entire spectrum, i.e., when we get a chirp with the IF values $f(t_1)$=0 and $f(t_2)=f_{max}$, where $[t_1, t_2]$ is the time interval considered in the LPFT calculation and f_{max} is the highest frequency in the LPFT spectrum. Binary masks obtained in the jammer excision procedure are given in Fig. 3. The obtained SNR_{out} curves are shown in Fig. 4(a) and (c), whereas the BER curves for the conventional and optimal case are shown in Fig. 4(b) and (d). Both the SNR_{out} and BER curves are functions of the chirp rate.

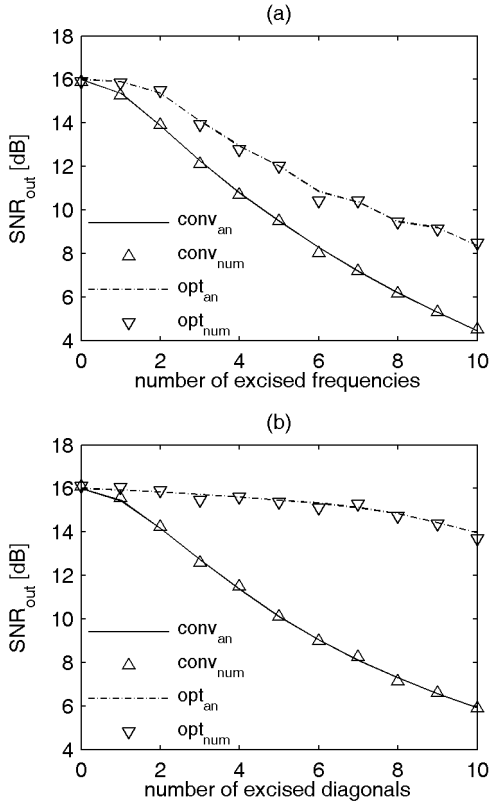

Fig. 2. Output SNR for the conventional (suboptimal) and the optimal receiver under the binary excision of the LPFT. Curves represent analytical results according to (31) . Triangles represent numerical values according to (12) over 20000 realizations.

Example 3: In this example, performances of the conventional and optimal STFT and LPFT receivers, when the desired signal is corrupted by a sinusoidal FM signal with variable amplitude of IF variation, are evaluated. The jammer is characterized by JSR=20dB and the amplitude of its sinusoidal IF law varies from 0 (a pure sinusoid in the middle of the spectrum) to the value at which it sweeps the entire frequency spectrum. Binary masks obtained in the jammer excision procedure are given in Fig. 5. The

obtained SNR_{out} curves are shown in Fig. 6(a) and (c), whereas the BER curves for the conventional and optimal case are shown in Fig. 6(b) and (d). Both the SNR_{out} and BER curves are functions of the amplitude of the sinusoidal IF law.

As Fig. 4 and 6 indicate, the optimal STFT and LPFT receivers exhibit significantly improved performances compared to the conventional ones. In addition, $LPFT_{opt}$ always gives the best results. It may seem unexpected that the SNR_{out} curves in the optimal LPFT case exhibit increasing trend (corresponding BER curves exhibit decreasing trend) as the jammer parameter increases in both examples. However, having in mind that, with the optimal LPFT receiver, the excised area in the t-f plane is approximately the same for all jammer parameter values [7], this ambiguity is partially resolved. Furthermore, for small parameter values, the jammer is nearly stationary, which corresponds to the frequencies excision case from the first example. By increasing the parameter value we are approaching the diagonals excision case, which is characterized by better performance of the receiver (see Fig. 2).

V. CONCLUSIONS

This paper has presented an optimal local polynomial Fourier transform approach for monocomponent jammer excision in DSSS communication systems. The LPFT is used to optimally concentrate the jammer in the t-f plane. The jammer excision is then obtained by removing its t-f signature via a binary mask. The binary mask inherently introduces a distortion of the received PN sequence; the decision making at the output of the receiver correlator is therefore suboptimal. The LPFT receiver is derived in matrix form and its optimization is performed by modifying the receiver PN sequence so that SNR_{out} is maximized. Performances of the conventional and optimal LPFT receivers are evaluated by simulations carried out on the received signal corrupted by monocomponent linear and sinusoidal FM jammers with variable parameters. The optimal LPFT receiver exhibits significantly improved performance compared to the conventional one, which is verified by analytically obtained (and numerically confirmed) SNR_{out} values and numerically computed BER values. The STFT receiver is considered as a special case of the LPFT receiver and its performance is assessed simultaneously with the performance of the LPFT receiver.

REFERENCES

[1] M. G. Amin, "Interference mitigation in spread spectrum communication systems using time-frequency distributions," *IEEE Trans. Signal Processing*, vol.45, pp. 90-101, Jan. 1997.

[2] C. Wang and M.G. Amin, "Performance analysis of instantaneous frequency-based interference excision techniques in spread spectrum communications," *IEEE Trans. Signal Processing*, vol. 46, pp. 70-82, Jan. 1998.

[3] X. Ouyang and M. G. Amin, "Short-time Fourier transform receiver for nonstationary interference excision in direct sequence spread spectrum communications," *IEEE Trans. Signal Processing*, vol.49, pp. 851-863, Apr. 2001.

[4] S. Barbarossa and A. Scaglione, "Adaptive time-varying cancellation of wideband interferences in spread-spectrum communications based on time-frequency distributions," *IEEE Trans. Signal Processing*, vol.47, pp. 957-965, Apr. 1999.

[5] O. Akay and F.G. Boudreaux-Bartels, "Broadband interference excision in spread spectrum communication systems via fractional Fourier transform," *Proc. Asilomar Conf. on Sig., Sys. and Comp.*, pp. 832-837, Nov. 1998.

[6] J. A. Young and J.S. Lehnert, "Analysis of DFT-based frequency excision algorithms for direct-sequence spread-spectrum communications," *IEEE Transactions on Communications*, vol. 46, no. 8, pp. 1076-1087, Aug. 1998.

[7] Lj. Stanković and S. Djukanović, "Order adaptive local polynomial FT based interference rejection in spread spectrum communication systems," *IEEE Transactions on Instrumentation and Measurement*, vol.54, pp. 2156-2162, Dec. 2005.

[8] S. Djukanović, M. Daković and Lj. Stanković, "Local polynomial Fourier transform receiver for nonstationary interference excision in DSSS communications", *IEEE Trans. Signal Process.*, vol. 56, No. 4, pp. 1627-1636, April 2008.

[9] J. Laster and J. Reed, "Interference rejection in digital wireless communication," *IEEE Signal Processing Mag*., pp. 37-62, May 1997.

[10] V. Katkovnik, "A new form of the Fourier transform for time-varying frequency estimation," *Signal Processing*, vol.47, no.2, pp. 187-200, 1995.

[11] V. Katkovnik, "Discrete-time local polynomial approximation of the instantaneous frequency," *IEEE Trans. Signal Processing*, vol.46, no.10, pp. 2626-2638, Oct. 1998.

[12] G. L. Stüber, *Principles of Mobile Communications*, Kluwer Academic Publishers, Massachusetts-USA, 2001.

[13] J. Ketchum and J. Proakis, "Adaptive algorithms for estimating and suppressing narrow band interference in PN spread spectrum systems," *IEEE Trans. on Communications*, vol. COM-30, pp. 913--924, May 1982.

[14] L. Milstein and R. Itlis, "Signal processing for interference rejection in spread spectrum communications," *IEEE Acoust., Speech, Signal Processing Mag*., vol. 3, pp. 18-31, Apr. 1986.

[15] A. Papoulis, *Probability, random variables, and stochastic processes*, 3rd edition, McGraw-Hill, New York, 1991.

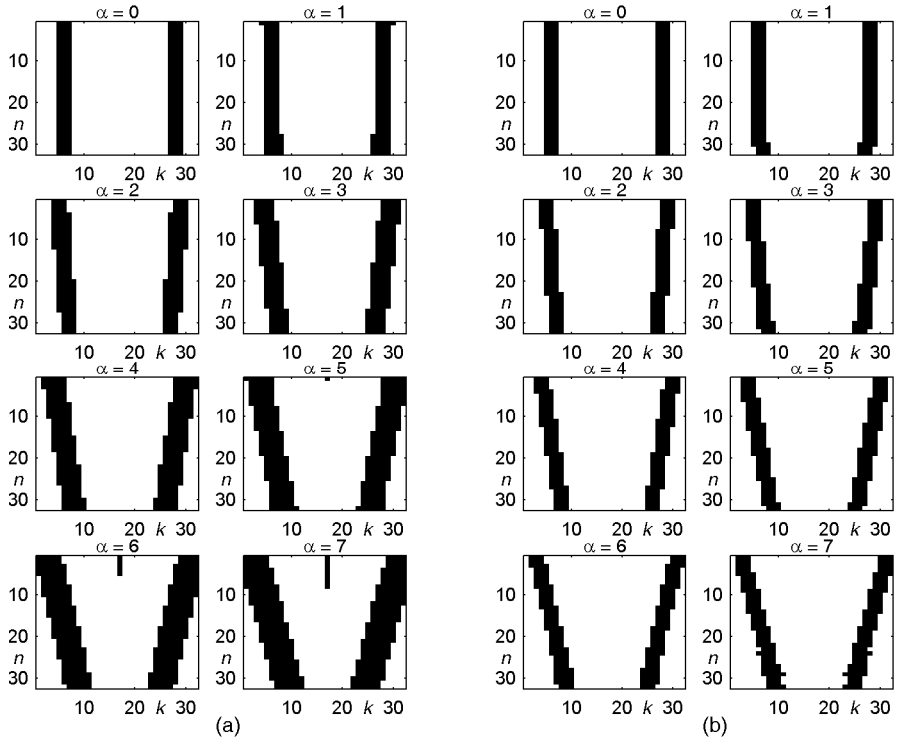

Fig. 3. Binary masks obtained in the linear FM jammer excision. α - variable chirp rate.

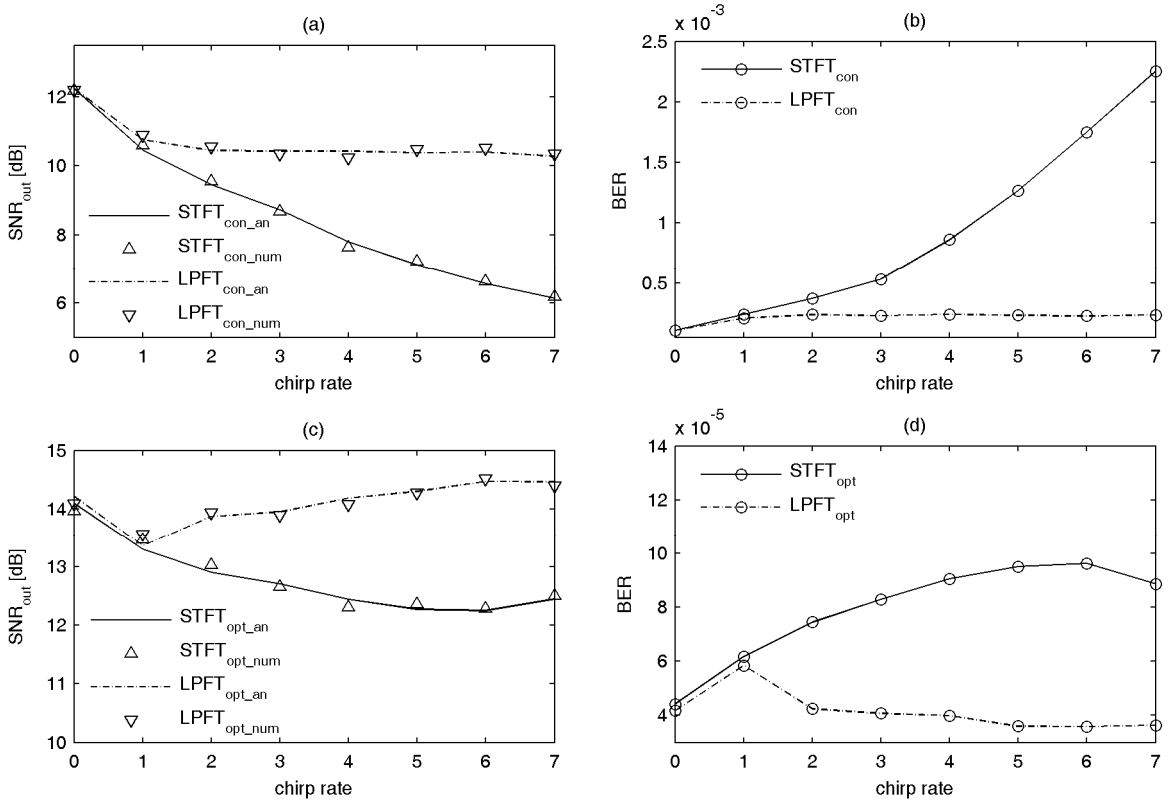

Fig. 4. Linear FM jammer case. *Left side*: Output SNR for (a) conventional and (c) optimal receivers. Curves represent analytical results according to (31). Triangles represent numerical values according to (12) over 20000 realizations. *Right side*: Numerical BER for (b) conventional and (d) optimal receivers.

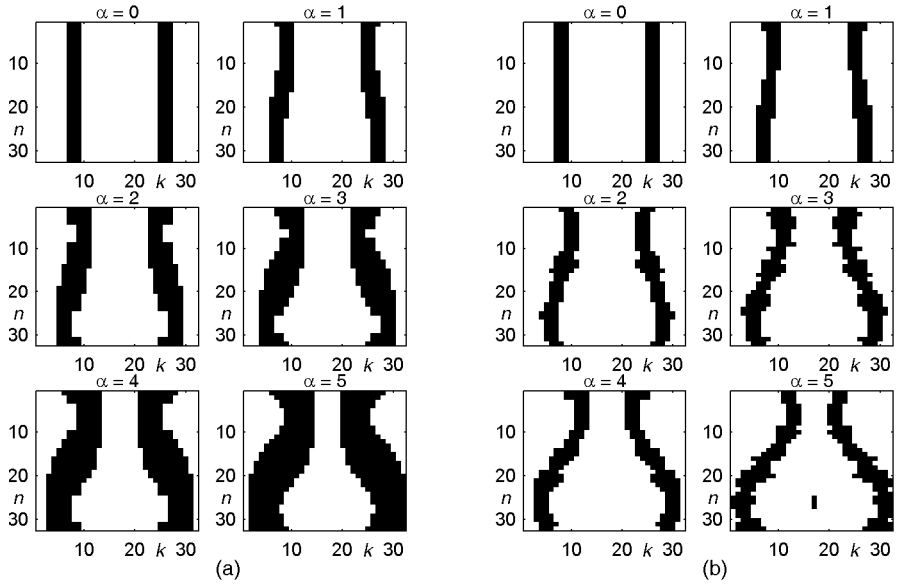

Fig. 5. Binary masks obtained in the sinusoidal FM jammer excision. α - variable amplitude of the sinusoidal IF law.

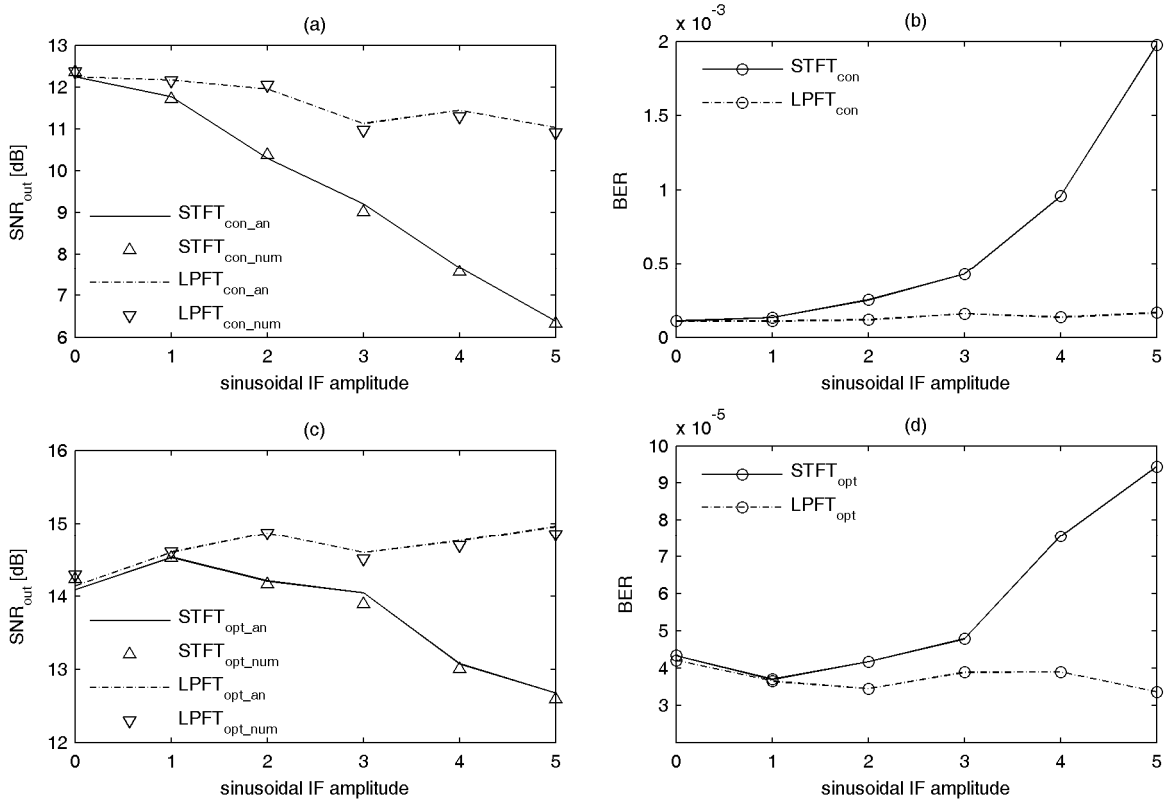

Fig. 6. Sinusoidal FM jammer case. *Left side*: Output SNR for (a) conventional and (c) optimal receivers. Curves represent analytical results according to (31). Triangles represent numerical values according to (12) over 20000 realizations. *Right side*: Numerical BER for (b) conventional and (d) optimal receivers.